Research Square

Preprints are preliminary reports that have not undergone peer review.
They should not be considered conclusive, used to inform clinical practice,
or referenced by the media as validated information.

HNRNPC Promotes Autophagy by Upregulating m6A-Modified FOXO1 Expression and Exacerbates the Progression of Rheumatoid Arthritis

Zhipeng Zeng
Nanchang University
Bowen Zheng
Nanchang University
Wen Ye
Nanchang University
Shiyu Gan
Nanchang University
Yang Yang
Nanchang University
Peng Yu
Nanchang University
Zhongbin Xia
408979872@qq.com
Nanchang University

Research Article

Keywords: Rheumatoid arthritis, HNRNPC, m6A modification, FOXO1, Autophagy

Posted Date: March 25th, 2026

DOI: https://doi.org/10.21203/rs.3.rs-8871975/v1

License: This work is licensed under a Creative Commons Attribution 4.0 International License.
Read Full License

Additional Declarations: No competing interests reported.

Abstract

Background

Rheumatoid arthritis (RA) is a systemic autoimmune disease characterized by synovial hyperplasia and chronic inflammation, whose molecular regulatory mechanisms are not fully elucidated. Both N6-methyladenosine (m6A) RNA modification and cellular autophagy are involved in the pathogenesis and progression of RA, but their synergistic regulatory mechanisms remain unclear.

Objective

To determine the expression profile of HNRNPC in RA and verify whether HNRNPC upregulates FOXO1 expression by stabilizing m6A-modified FOXO1 mRNA, thereby activating autophagy in MH7A cells and promoting RA inflammatory progression.

Methods

Bioinformatics analysis was performed based on the RA-related dataset GSE93776 from the GEO database to screen differentially expressed m6A regulators and construct a diagnostic model. An in vitro RA cell model was established by stimulating human synovial fibroblast cell line MH7A with tumor necrosis factor-α (TNF-α). MeRIP-qPCR was used to detect the m6A modification level of FOXO1 mRNA. RIP-qPCR was performed to validate the direct binding between HNRNPC and FOXO1 mRNA. siRNA-mediated knockdown of HNRNPC or overexpression of FOXO1 was employed, combined with qRT-PCR, Western blot, CCK-8, and immunofluorescence techniques to analyze the regulatory effects of HNRNPC on FOXO1 expression, MH7A cell viability, and autophagy. Rescue experiments were conducted to verify the specificity of this regulatory axis.

Results

 Bioinformatics analysis revealed that HNRNPC was significantly overexpressed in RA and was the most crucial m6A regulator for distinguishing RA from normal samples (highest Mean Decrease Gini value). In the RA cell model, both mRNA and protein expression levels of HNRNPC and FOXO1 were significantly upregulated. The m6A modification level of FOXO1 mRNA was increased compared to the control group. Knockdown of HNRNPC significantly reduced the m6A modification level of FOXO1. RIP experiments confirmed that HNRNPC could directly bind to FOXO1 mRNA. Actinomycin D experiments indicated that HNRNPC knockdown shortened the half-life of FOXO1 mRNA, reducing its stability and protein expression. Knockdown of HNRNPC inhibited autophagy activation in MH7A cells, manifested as decreased LC3-II/I ratio and Beclin1 expression, reduced number of autophagic flux fluorescent puncta, and suppression of abnormal MH7A cell proliferation. Rescue experiments confirmed that

overexpression of FOXO1 could partially reverse the autophagy inhibition and decreased cell viability caused by HNRNPC knockdown.

Conclusion

This study reveals for the first time a novel regulatory axis in RA: HNRNPC ↑ → m6A-modified FOXO1 mRNA stabilization → FOXO1 expression ↑ → MH7A cell autophagy activation → RA inflammatory progression ↑. It identifies HNRNPC as a key m6A regulator in RA, providing a new molecular target and theoretical basis for targeted RA therapy.

1.Introduction

Rheumatoid arthritis (RA) is a chronic, systemic autoimmune disease characterized primarily by chronic inflammation, hyperplasia of synovial tissue, and progressive joint destruction, ultimately leading to disability (1). Abnormal activation of fibroblast-like synoviocytes (FLS) is a core pathological event in RA, exhibiting properties such as invasive growth, anti-apoptosis, and high secretion of inflammatory factors (2). Current RA treatments focus on anti-inflammatory and immunosuppressive agents, but some patients show poor response. The precise molecular regulatory mechanisms of the disease are not fully understood; therefore, identifying core molecular targets in RA pathogenesis and elucidating their regulatory mechanisms hold significant clinical importance.

N6-methyladenosine (m6A) is the most prevalent post-transcriptional modification in eukaryotic mRNA. It is dynamically regulated by a system comprising methyltransferases ("Writers," e.g., METTL3/14), demethylases ("Erasers," e.g., FTO, ALKBH5), and reader proteins ("Readers," e.g., YTHDF family, HNRNPC), influencing RNA stability, translation, and splicing in various biological processes (3, 4). Recent studies indicate that m6A regulators are aberrantly expressed in peripheral blood and synovial tissues of RA patients, and their modification patterns are closely associated with the RA immune microenvironment (5–7). Heterogeneous nuclear ribonucleoprotein C (HNRNPC), as a classical m6A reader protein, recognizes m6A modification-induced RNA structural changes and binds target mRNAs, regulating their degradation and translation (8). Previous studies found it overexpressed in various cancers promoting disease progression (9), but its role and molecular mechanism in RA have not been reported.

Forkhead box protein O1 (FOXO1) is a key transcription factor regulating cell cycle, apoptosis, and autophagy. In RA, it promotes angiogenesis and abnormal activation of synovial cells (10, 11), and its expression is regulated by m6A modification (12). Autophagy is a crucial process for cellular degradation and recycling of intracellular components. In RA, autophagy levels in synovial cells are abnormally elevated, closely linked to cell anti-apoptosis, inflammatory cytokine secretion, and joint destruction (13–15). FOXO1 has been confirmed to mediate autophagy activation in various cell types(16, 17), but its upstream regulatory mechanisms in RA-relevant cell models remain unclear.

Based on the above background, we propose the scientific hypothesis: In RA, the overexpressed HNRNPC, as an m6A reader, recognizes and stabilizes m6A-modified FOXO1 mRNA, upregulates FOXO1 protein expression, thereby activating autophagy in MH7A cells, ultimately promoting RA inflammatory progression. This study integrates bioinformatics analysis and in vitro cell experiments to systematically verify this regulatory axis, providing a theoretical basis for understanding RA pathogenesis and developing new therapeutic strategies.

2. Materials and Methods

2.1 Bioinformatics Analysis

The RA gene expression dataset GSE93776 (containing 173 samples) was downloaded from the Gene Expression Omnibus (GEO) database. Expression data for 23 known m6A regulators (7 Writers, 2 Erasers, 12 Readers) were extracted. Differential expression analysis was performed using the Wilcoxon rank-sum test (screening criteria: $P < 0.05$). Protein-protein interaction (PPI) network was constructed using the STRING database (confidence > 0.7) and visualized with Cytoscape software. Random Forest (RF) and Support Vector Machine (SVM) models were built using the "randomForest" and "e1071" packages in R, respectively. Model residual analysis was performed using the "DALEX" package. The importance of feature factors was evaluated by the Mean Decrease Gini index.

Based on the screened differentially expressed m6A regulators, unsupervised consensus clustering of RA samples was performed using the "ConsensusClusterPlus" package to determine the optimal cluster number and define m6A modification subtypes. An m6A score model was constructed based on principal component analysis (PCA) using the formula: m6A Score=$\sum$(PC1i+PC2i). Differentially expressed genes (DEGs) between different m6A subtypes were identified using the "limma" package (screening criteria: $P < 0.05$, $|\log2FC|>0.5$). Gene Ontology (GO) and Kyoto Encyclopedia of Genes and Genomes (KEGG) pathway enrichment analyses were performed using the "clusterProfiler" package.

The infiltration scores of 28 immune cell types were calculated using single-sample gene set enrichment analysis (ssGSEA). Spearman correlation analysis and Mantel test were used to assess the association among m6A score, HNRNPC expression, and immune infiltration. The intersection of DEGs between RA and normal samples and DEGs between m6A subtypes was obtained. Diagnostic biomarkers were screened via LASSO regression (10-fold cross-validation) and used to construct a nomogram model. The diagnostic efficacy of the model in the training and validation sets was evaluated using receiver operating characteristic (ROC) curves.

2.2 Cell Culture and RA Model Establishment

The human synovial fibroblast cell line MH7A was purchased from the Cell Bank of the Chinese Academy of Sciences and cultured in DMEM high-glucose medium supplemented with 10% fetal bovine serum and 1% penicillin-streptomycin at 37°C in a 5% CO2 incubator. Cells in the logarithmic growth phase were stimulated with 1 ng/mL recombinant human TNF-α for 24 h to establish the in vitro RA

inflammation model. The control group received an equal volume of PBS. The optimal stimulation concentration was determined via TNF-α concentration gradient experiments (0, 1, 5, 10, 20, 40 ng/mL).

2.3 Cell Transfection

Three siRNAs targeting HNRNPC (si-HNRNPC-1/2/3) and negative control siRNA (si-NC) were designed and synthesized by Shanghai GenePharma. The FOXO1 overexpression plasmid (pcDNA3.1-FOXO1) and empty vector control (pcDNA3.1) were provided by Guangzhou Fulengen. Transfection was performed using Lipofectamine 3000 transfection reagent according to the manufacturer's instructions. Transfection groups were: siNC group, siHNRNPC group, pcDNA3.1 group, pcDNA3.1-FOXO1 group, siHNRNPC+pcDNA3.1 group, siHNRNPC+pcDNA3.1-FOXO1 group. Cells were collected 48 h post-transfection, and transfection efficiency was verified by qRT-PCR and Western blot.

2.4 Quantitative Real-Time PCR (qRT-PCR)

Total RNA was extracted using TRIzol reagent. RNA concentration and purity (A260/A280 = 1.85 ~ 2.05) were measured using NanoDrop 2000. cDNA was synthesized using the PrimeScript RT reagent Kit. qRT-PCR was performed using SYBR Premix Ex Taq II on the LightCycler 480 II system. Reaction conditions: 95°C for 30 s pre-denaturation; 40 cycles of 95°C for 5 s, 60°C for 30 s. GAPDH served as the internal control. Relative gene expression was calculated using the $2 - \Delta\Delta Ct$ method. Primer sequences are listed in **Supplement 1.**.

2.5 Western Blot Analysis

Total protein was extracted using RIPA lysis buffer containing protease inhibitors. Protein concentration was determined using the BCA method. Equal amounts of protein were separated by SDS-PAGE and transferred onto PVDF membranes. Membranes were blocked with 5% skimmed milk for 1 h, followed by incubation with primary antibodies (anti-HNRNPC, anti-FOXO1, anti-LC3B, anti-Beclin1, anti-β-actin) overnight at 4°C. After washing with TBST, membranes were incubated with HRP-conjugated secondary antibodies at room temperature for 1 h. Protein bands were visualized using ECL ultrasensitive luminescence solution and captured using a Tanon 5200 imaging system. Band intensity was analyzed using ImageJ software. Relative protein expression was normalized to β-actin.

2.6 RNA Immunoprecipitation (RIP)

The Magna RIP RNA-Binding Protein Immunoprecipitation Kit was used. Approximately 1×10^7 MH7A cells were collected and lysed with RIP lysis buffer. 10% of the lysate was saved as Input control. The remaining lysate was incubated overnight at 4°C with magnetic beads coated with anti-HNRNPC antibody or control IgG. After washing, the immunoprecipitated complexes were digested with Proteinase K. RNA was extracted and subjected to qRT-PCR to detect the relative enrichment of FOXO1 mRNA in the immunoprecipitated products.

2.7 m6A Methylated RNA Immunoprecipitation (MeRIP-qPCR)

The EpiQuik CUT&RUN m6A RNA Enrichment Kit was used to detect the m6A modification level of FOXO1 mRNA. Total RNA was extracted and fragmented to 100–200 nt. 10% of the fragmented RNA was saved as Input control. The remaining RNA was immunoprecipitated with anti-m6A antibody at 4°C. The enriched RNA fragments were purified and subjected to qRT-PCR. The ratio of FOXO1 mRNA in the m6A-IP products to the Input was calculated.

2.8 mRNA Stability Assay (Actinomycin D Experiment)

Forty-eight hours after transfection with si-NC or si-HNRNPC, cells were treated with actinomycin D at a final concentration of 2 μg/mL to inhibit new RNA synthesis. Cells were collected at 0, 2, 4, 6, 8 h. Total RNA was extracted, and FOXO1 mRNA remaining levels were detected by qRT-PCR. The 0 h expression level was set as 100% to plot mRNA decay curves. mRNA half-life was calculated using a one-phase exponential decay model.

2.9 Cell Viability Assay (CCK-8)

MH7A cells were seeded into 96-well plates at a density of 5×10^3 cells per well. After respective treatments, 10 μL of CCK-8 solution was added to each well, followed by incubation at 37°C for 2 h. Absorbance (OD) at 450 nm was measured using a multimode microplate reader. Each group contained five replicate wells.

2.10 Immunofluorescence Detection of Autophagic Flux

Cells were co-transfected with GFP-LC3B and mCherry-LC3B plasmids for 24 h, then treated accordingly. Cells were fixed with 4% paraformaldehyde for 15 min and nuclei were stained with DAPI. Images were captured using a laser scanning confocal microscope. For each sample, 20 cells were randomly selected, and the numbers of yellow ($GFP^+mCherry^+$, autophagosomes) and red ($GFP^-mCherry^+$, autolysosomes) fluorescent puncta were counted in a blinded manner. Autophagic flux score was calculated as (total puncta number / cell).

2.11 Statistical Analysis

All in vitro experiments were independently repeated three times. Statistical analysis was performed using GraphPad Prism 9.0 software. Data are presented as mean ± standard deviation. Comparisons between two groups were analyzed using unpaired Student's t-test. Comparisons among multiple groups were analyzed by one-way analysis of variance (ANOVA), followed by Tukey's post hoc test when variances were homogeneous. Time-series data were analyzed using two-way ANOVA. P-values in bioinformatics analysis were adjusted for multiple testing. $P < 0.05$ was considered statistically significant.

3. Results

3.1 Bioinformatics Analysis Identifies HNRNPC as a Key Overexpressed m6A Regulator in RA

We analyzed the GEO dataset GSE93776 to systematically evaluate the roles of 23 known m6A regulators in RA. Differential expression analysis showed that compared to normal samples, four factors (HNRNPC, METTL3, ZC3H13, FMR1) were significantly upregulated in RA samples, with HNRNPC showing the most significant differential expression (log2FC = 1.83, P = 2.3e-11, Fig. 1B). Spearman correlation analysis revealed significant co-expression relationships among the 23 m6A regulators, with HNRNPC showing strong positive correlations with METTL3 and WTAP ($r > 0.6$, $P < 0.001$, Fig. 1A). PPI network analysis showed that HNRNPC directly interacted with core m6A regulators (METTL3, WTAP), positioning it at a key node in the m6A regulatory network (Fig. 1C).

To evaluate the diagnostic value of these factors for RA, we constructed Random Forest (RF) and Support Vector Machine (SVM) models. DALEX residual analysis indicated a better fit for the RF model (Fig. 6A-B). ROC curve analysis also confirmed that the diagnostic performance of the RF model was significantly higher than that of the SVM model (AUC: RF 1.000 vs. SVM 0.827) (Fig. 6C). The error rate trend plot of the RF model showed that the out-of-bag (OOB) error rate stabilized at 5.2% when the number of decision trees reached 100 (Fig. 6D). Feature importance ranking indicated that HNRNPC had the highest Mean Decrease Gini value (4.87, Fig. 1D), making it the core feature distinguishing RA from normal samples. In the nomogram diagnostic model constructed based on the four key m6A regulators, HNRNPC had the highest score weight (8.2 points, Fig. 6E). The calibration curve showed good agreement between the predicted probability and the actual disease probability, with a consistency index (C-index) of 0.92, indicating good clinical applicability (Fig. 6F).

Based on the expression profiles of these four key factors, RA patient samples were divided into two m6A modification subtypes (Cluster A and Cluster B) via unsupervised consensus clustering. The consensus clustering CDF curve and the rate of change of the area under the CDF curve indicated $K = 2$ as the optimal cluster number (Fig. 7A-B). The consensus matrix heatmap showed good clustering stability (Fig. 7D). PCA analysis revealed significant separation between the two subtypes (separation degree = 0.91, Fig. 7C). The four key m6A regulators were expressed significantly higher in Cluster B than in Cluster A (Fig. 7E).

Functional enrichment analysis showed that the DEGs between the two m6A subtypes were mainly enriched in GO biological processes such as immune response, inflammatory response, and leukocyte migration (Fig. 7F). KEGG pathway enrichment analysis showed enrichment in inflammation-related pathways such as rheumatoid arthritis, Th17 cell differentiation, and inflammatory bowel disease (Fig. 7G). These bioinformatics findings collectively highlight HNRNPC as a key, overexpressed m6A regulator in RA, prompting our subsequent functional investigations in a relevant cellular model.

3.2 HNRNPC and FOXO1 Are Upregulated and FOXO1 m6A Modification Is Enhanced in the RA Cell Model

To validate the bioinformatics findings, we stimulated MH7A cells with 1 ng/mL TNF-α to establish the in vitro RA model. qRT-PCR analysis showed that the mRNA expression of the inflammatory cytokine IL-1B was significantly increased ($P < 0.001$, Fig. 2A), confirming successful establishment of the RA cell

model. TNF-α concentration gradient experiments showed that 1 ng/mL TNF-α induced the highest level of HNRNPC mRNA expression (relative expression = 3.12 ± 0.28, P < 0.001, Fig. 2B), which was determined as the optimal concentration for subsequent experiments.

At the protein level, Western blot results showed that compared to the control group, the protein expression levels of both HNRNPC and FOXO1 were significantly upregulated in the RA model group (HNRNPC: 2.05 ± 0.21-fold, FOXO1: 1.87 ± 0.19-fold, P < 0.01, Fig. 2D-E). Knockdown of HNRNPC significantly decreased FOXO1 protein expression (0.63 ± 0.09-fold, P < 0.001, Fig. 2E). MeRIP-qPCR experiments showed that the m6A modification level of FOXO1 mRNA was significantly higher in the RA model group than in the control group (% Input: 0.72 ± 0.08 vs 0.21 ± 0.03, P < 0.001). Knockdown of HNRNPC significantly reduced its m6A modification level (0.35 ± 0.04, P < 0.01, Fig. 2F). RNA quality assessment indicated that RNA purity, integrity, and fragment length met experimental requirements (Fig. 2C). These results confirmed that under RA inflammatory conditions, HNRNPC and FOXO1 expressions were concurrently upregulated, and the m6A modification level of FOXO1 was enhanced.

3.3 HNRNPC Directly Binds to m6A-Modified FOXO1 mRNA and Enhances Its Stability

RIP-qPCR experiments confirmed the direct binding between HNRNPC and FOXO1 mRNA. Compared to the IgG control group, the anti-HNRNPC antibody group specifically enriched FOXO1 mRNA (% Input: 1.28 ± 0.15 vs 0.12 ± 0.03, P < 0.001). Agarose gel electrophoresis showed no non-specific amplification in the experiment, and GAPDH served as a negative control without enrichment (Fig. 3A).

We used siRNA to knockdown HNRNPC expression. qRT-PCR analysis showed that all three siRNAs effectively knocked down HNRNPC, with si-HNRNPC-3 having the highest knockdown efficiency (79%, relative expression = 0.21 ± 0.03, P < 0.001, Fig. 3B). The qRT-PCR and melt curve results for knockdown efficiency showed single peaks for all samples, with no primer dimers or non-specific amplification, verifying the specificity of the qPCR experiments (Fig. 8A-C). Following HNRNPC knockdown, FOXO1 mRNA expression decreased in a gradient manner corresponding to the knockdown efficiency, with the si-HNRNPC-3 group showing the lowest FOXO1 mRNA expression (0.43 ± 0.05, P < 0.001, Fig. 3C). Their expression levels showed a significant positive correlation (r = 0.89, P < 0.01).

To elucidate the regulatory mechanism, we performed actinomycin D experiments. Results showed that after HNRNPC knockdown, the degradation rate of FOXO1 mRNA significantly accelerated, with its half-life shortened from 6.5 ± 0.4 h in the control group to 3.2 ± 0.3 h (P < 0.01, Fig. 3D-F). Melt curves showed single peaks, confirming the absence of non-specific amplification in qPCR detection (Fig. 3E), suggesting that HNRNPC upregulates FOXO1 expression by enhancing its mRNA stability.

3.4 Knockdown of HNRNPC Inhibits Autophagy and Abnormal Proliferation in MH7A Cells

Given that FOXO1 is a known regulator of autophagy, we further investigated the effect of HNRNPC on autophagy in MH7A cells. Immunofluorescence double-labeling for autophagic flux showed that in the RA model group, the numbers of $GFP^{+}mCherry^{+}$ (yellow) and $GFP^{-}mCherry^{+}$ (red) puncta in MH7A cells were significantly increased, and the autophagic flux score was elevated. Knockdown of HNRNPC significantly reduced the number of autophagic fluorescent puncta and markedly inhibited autophagic flux (Fig. 4A). Western blot results showed that knockdown of HNRNPC significantly downregulated the expression of the key autophagy protein Beclin1 and the LC3-II/I ratio in MH7A cells ($P < 0.01$, Fig. 4C), consistent with the immunofluorescence results.

CCK-8 assays showed that cell viability in the RA model group was significantly higher than in the control group (OD450: 1.87 ± 0.12 vs 1.00 ± 0.07, $P < 0.001$). Knockdown of HNRNPC significantly reduced cell viability (1.15 ± 0.08, $P < 0.001$). Overexpression of FOXO1 partially rescued the decrease in cell viability caused by HNRNPC knockdown (OD450 recovered to 1.56 ± 0.10, $P < 0.01$, Fig. 4B).

3.5 FOXO1 Overexpression Partially Reverses Autophagy Inhibition Caused by HNRNPC Knockdown

To confirm that HNRNPC affects autophagy by regulating FOXO1, we performed rescue experiments. Results from qRT-PCR and melt curve validation of the FOXO1 overexpression vector showed that FOXO1 mRNA expression in the OE-FOXO1 group was 1520-fold higher than in the OE-NC group ($P < 0.001$). The melt curve showed a single peak, confirming no ectopic transcription from the overexpression vector (Fig. 8D-F). Compared to the siHNRNPC+pcDNA3.1 group, FOXO1 protein expression was significantly restored in the siHNRNPC+pcDNA3.1-FOXO1 group (0.82 ± 0.07 vs 0.38 ± 0.05, $P < 0.001$, Fig. 5B). Concurrently, the expression of the key autophagy protein Beclin1 and the LC3-II/I ratio were significantly upregulated ($P < 0.01$, Fig. 5B).

Immunofluorescence double-labeling results showed that the number of autophagic flux fluorescent puncta was significantly lower in the HNRNPC knockdown group compared to the control group. After FOXO1 overexpression, the number of autophagic puncta showed some recovery, with a rescue efficiency of 65% ($P < 0.01$, Fig. 5A). These results confirm that FOXO1 is the key downstream effector molecule through which HNRNPC regulates autophagy in MH7A cells. HNRNPC activates MH7A cell autophagy by upregulating FOXO1 expression.

4. Discussion

This study, by integrating bioinformatics analysis and systematic in vitro cell experiments, reveals for the first time the central role of the HNRNPC/m6A-FOXO1-autophagy regulatory axis in MH7A cell activation and inflammatory progression in rheumatoid arthritis (RA), providing a new perspective for RA molecular mechanism research. The core findings include: HNRNPC is specifically overexpressed in RA patients and cell models, serving as a key m6A regulator. As an m6A reader protein, it upregulates FOXO1 expression by recognizing and stabilizing m6A-modified FOXO1 mRNA. This ultimately activates MH7A cell autophagy, promotes abnormal cell proliferation, and exacerbates RA pathological progression. The

discovery of this regulatory axis not only refines the molecular network of synergistic regulation between m6A modification and autophagy in RA but also provides potential dual-action targets for targeted RA therapy.

4.1 Expression Characteristics and Clinical Significance of HNRNPC in RA

HNRNPC, as a classical m6A reader protein, primarily functions to recognize m6A-modified RNA and regulate its fate. Previous research has mostly focused on cancer, confirming its role in promoting tumor progression by stabilizing target gene mRNAs (8, 9, 18–20). This study, through bioinformatics analysis, is the first to clearly demonstrate that HNRNPC is significantly overexpressed in peripheral blood samples from RA patients. In the Random Forest model, it had the highest feature importance score (Mean Decrease Gini = 4.87), making it the core m6A regulator distinguishing RA from normal samples. This bioinformatics finding directed our subsequent cellular investigation. In vitro cell experiments further confirmed that TNF-α-induced RA inflammatory environment concentration-dependently upregulated HNRNPC expression, with its expression peaking at 1 ng/mL TNF-α stimulation. This clearly establishes a positive correlation between HNRNPC expression and RA inflammation severity, laying a pathological association foundation for subsequent mechanistic studies.

4.2 Innovation in the Molecular Mechanism of HNRNPC Regulating FOXO1

The core biological function of m6A modification is to regulate the stability, translation, or degradation of target mRNAs through reader proteins. Previous research has mostly focused on the regulation of FOXO1 m6A modification by methyltransferases (e.g., METTL14) (12, 21–23). This study is the first to link m6A reader proteins to the post-transcriptional regulation of FOXO1, thereby refining the m6A modification regulatory network of FOXO1. MeRIP-qPCR experiments confirmed that the m6A modification level of FOXO1 mRNA was significantly increased in MH7A cells, and knockdown of HNRNPC significantly reduced its m6A enrichment. RIP-qPCR experiments directly confirmed the specific binding between HNRNPC and FOXO1 mRNA. Actinomycin D experiments further clarified that HNRNPC enhances the stability of FOXO1 mRNA by prolonging its half-life (from 6.5 ± 0.4 h to 3.2 ± 0.3 h), thereby upregulating its transcriptional and translational levels. This mechanism reveals a novel post-transcriptional regulatory mode for the abnormal overexpression of pathogenic genes in RA—m6A modification-mediated mRNA stability regulation—providing a new entry point for understanding RA molecular pathology.

4.3 Pathological Role and Therapeutic Potential of Autophagy in the Regulatory Axis

The role of autophagy in RA exhibits a significant duality: moderate autophagy maintains cellular homeostasis, while excessive autophagy promotes abnormal activation, anti-apoptosis, and joint

destruction of synovial cells (13, 14, 24, 25). This study confirms that autophagy levels are significantly elevated in MH7A cells, manifested as enhanced autophagic flux, upregulated Beclin1 expression, and increased LC3-II/I ratio. Knockdown of HNRNPC significantly inhibited autophagy activation by downregulating FOXO1 expression. Rescue experiments further confirmed that FOXO1 is the key downstream molecule through which HNRNPC regulates autophagy. Overexpression of FOXO1 partially reversed the autophagy inhibition and abnormal cell proliferation caused by HNRNPC knockdown. This result clarifies the linear regulatory cascade of HNRNPC → FOXO1 → autophagy, directly linking m6A modification for the first time to abnormal autophagy activation in a RA-relevant cellular model, revealing a novel molecular mechanism in RA pathogenesis. More importantly, knockdown of HNRNPC not only inhibited autophagy but also directly suppressed the proliferation of MH7A cells, suggesting that targeting HNRNPC may intervene in RA progression through a dual mechanism of "inhibiting autophagy + blocking cell proliferation," offering a new strategic direction for RA treatment.

4.4 Study Limitations and Future Perspectives

Although this study systematically validated the functionality of the HNRNPC/m6A-FOXO1-autophagy regulatory axis, certain limitations remain: Conclusions are primarily based on in vitro cell models. While bioinformatics analysis and preliminary observations in CIA mice suggest trends in HNRNPC and FOXO1 expression, complete in vivo functional validation using joint-specific knockout/overexpression is pending. Subsequent animal experiments are needed to confirm the in vivo validity of this regulatory axis. The specific m6A modification sites on FOXO1 mRNA and the binding domains of HNRNPC have not been identified. Point mutation experiments, RNA pull-down assays, etc., are needed to further dissect the molecular details of their interaction. This study focused on FOXO1 as a single target gene. As an m6A reader protein, HNRNPC may regulate multiple downstream targets. Whether it cooperatively regulates RA inflammatory progression through multiple targets requires further exploration. The association between this regulatory axis and RA clinical phenotypes (e.g., disease activity, joint destruction severity) was not explored. Future studies need to expand clinical sample sizes to validate the diagnostic and prognostic evaluation value of HNRNPC.

5. Conclusion

Through bioinformatics analysis and in vitro cell experiments, this study identified HNRNPC as a key overexpressed m6A regulator in RA for the first time. It revealed a novel molecular regulatory axis: HNRNPC ↑ → m6A-modified FOXO1 mRNA stabilization → FOXO1 expression ↑ → MH7A cell autophagy activation → RA inflammatory progression ↑. This research not only deepens the understanding of RA pathogenesis but also provides new molecular targets and a theoretical basis for RA diagnosis and targeted therapy. Subsequent in vivo validation of this regulatory axis and the development of targeted drugs hold promise for bringing new therapeutic options to RA patients.

Declarations

Acknowledgments

None.

Ethics approval and consent to participate

None.

Consent for publication

Not applicable.

Availability of data and materials

The data used to support the findings of this study are available from the corresponding author upon reasonable request.

Competing interests

All authors certify that they have no affiliations with or involvement in any organization or entity with any financial interest or non-financial interest in the subject matter or materials discussed in this manuscript.

Funding

This work was supported by the Jiangxi Provincial Science and Technology Department Natural Science Foundation, Youth Fund Project 20242BAB20387.

Author Contributions Statement

Z.P.Z.: Investigation, Validation, Writing – Review & Editing.

B.W.Z.: Investigation, Methodology, Formal Analysis.

W.Y.: Writing – Original Draft, Visualization, Data Curation.

S.Y.G.: Resources, Validation.

Y.Y.: Software, Formal Analysis.

P.Y.: Supervision, Funding Acquisition, Writing – Review & Editing.

Z.B.X.: Conceptualization, Supervision, Project Administration, Funding Acquisition, Data Curation, Writing – Review & Editing.

All authors critically reviewed and approved the final manuscript.

References

1. Smolen JS, Aletaha D, McInnes IB. Rheumatoid arthritis. Lancet. 2016;388(10055):2023–38. Epub 2016/10/30. doi: 10.1016/s0140-6736(16)30173-8. PubMed PMID: 27156434.
2. Bartok B, Firestein GS. Fibroblast-like synoviocytes: key effector cells in rheumatoid arthritis. Immunol Rev. 2010;233(1):233 – 55. Epub 2010/03/03. doi: 10.1111/j.0105-2896.2009.00859.x. PubMed PMID: 20193003; PubMed Central PMCID: PMCPMC2913689.
3. Zaccara S, Ries RJ, Jaffrey SR. Publisher Correction: Reading, writing and erasing mRNA methylation. Nat Rev Mol Cell Biol. 2023;24(10):770. Epub 2023/08/22. doi: 10.1038/s41580-023-00654-3. PubMed PMID: 37604996.
4. Shi H, Wei J, He C. Where, When, and How: Context-Dependent Functions of RNA Methylation Writers, Readers, and Erasers. Mol Cell. 2019;74(4):640–50. Epub 2019/05/18. doi: 10.1016/j.molcel.2019.04.025. PubMed PMID: 31100245; PubMed Central PMCID: PMCPMC6527355.
5. Song S, Zhao R, Qiao J, Liu J, Cheng T, Zhang SX, et al. Predictive value of drug efficacy by M6A modification patterns in rheumatoid arthritis patients. Front Immunol. 2022;13:940918. Epub 2022/09/03. doi: 10.3389/fimmu.2022.940918. PubMed PMID: 36052084; PubMed Central PMCID: PMCPMC9427021.
6. Ma C, Wu J, Lei H, Huang H, Li Y. Significance of m6A in subtype identification, immunological evolution, and therapeutic sensitivity of RA. Immunobiology. 2024;229(1):152781. Epub 2023/12/29. doi: 10.1016/j.imbio.2023.152781. PubMed PMID: 38154164.
7. Wang F, Wen J, Liu J, Xin L, Fang Y, Sun Y, et al. Demethylase FTO mediates m6A modification of ENST00000619282 to promote apoptosis escape in rheumatoid arthritis and the intervention effect of Xinfeng Capsule. Front Immunol. 2025;16:1556764. Epub 2025/04/04. doi: 10.3389/fimmu.2025.1556764. PubMed PMID: 40181982; PubMed Central PMCID: PMCPMC11966437.
8. Liu N, Zhou KI, Parisien M, Dai Q, Diatchenko L, Pan T. N6-methyladenosine alters RNA structure to regulate binding of a low-complexity protein. Nucleic Acids Res. 2017;45(10):6051–63. Epub 2017/03/24. doi: 10.1093/nar/gkx141. PubMed PMID: 28334903; PubMed Central PMCID: PMCPMC5449601.
9. Zhou KI, Shi H, Lyu R, Wylder AC, Matuszek Ż, Pan JN, et al. Regulation of Co-transcriptional Pre-mRNA Splicing by m(6)A through the Low-Complexity Protein hnRNPG. Mol Cell. 2019;76(1):70–81.e9. Epub 2019/08/26. doi: 10.1016/j.molcel.2019.07.005. PubMed PMID: 31445886; PubMed Central PMCID: PMCPMC6778029.
10. Nagata Y, Nakasa T, Mochizuki Y, Ishikawa M, Miyaki S, Shibuya H, et al. Induction of apoptosis in the synovium of mice with autoantibody-mediated arthritis by the intraarticular injection of double-stranded MicroRNA-15a. Arthritis Rheum. 2009;60(9):2677–83. Epub 2009/08/29. doi: 10.1002/art.24762. PubMed PMID: 19714650.
11. Zhang J, Ma Y, Zhang Y, Niu S, Chu M, Zhang Z. Angiogenesis is Inhibited by Arsenic Trioxide Through Downregulation of the CircHIPK3/miR-149-5p/FOXO1/VEGF Functional Module in

Rheumatoid Arthritis. Front Pharmacol. 2021;12:751667. Epub 2021/11/16. doi: 10.3389/fphar.2021.751667. PubMed PMID: 34776969; PubMed Central PMCID: PMCPMC8579003.

12. Ye M, Chen J, Lu F, Zhao M, Wu S, Hu C, et al. Down-regulated FTO and ALKBH5 co-operatively activates FOXO signaling through m6A methylation modification in HK2 mRNA mediated by IGF2BP2 to enhance glycolysis in colorectal cancer. Cell Biosci. 2023;13(1):148. Epub 2023/08/15. doi: 10.1186/s13578-023-01100-9. PubMed PMID: 37580808; PubMed Central PMCID: PMCPMC10424385.
13. Kato M, Ospelt C, Gay RE, Gay S, Klein K. Dual role of autophagy in stress-induced cell death in rheumatoid arthritis synovial fibroblasts. Arthritis Rheumatol. 2014;66(1):40–8. Epub 2014/01/23. doi: 10.1002/art.38190. PubMed PMID: 24449574.
14. Zhou W, Shen Q, Wang H, Yang J, Zhang C, Deng Z, et al. Knockdown of YAP/TAZ Inhibits the Migration and Invasion of Fibroblast Synovial Cells in Rheumatoid Arthritis by Regulating Autophagy. J Immunol Res. 2020;2020:9510594. Epub 2020/11/05. doi: 10.1155/2020/9510594. PubMed PMID: 33145365; PubMed Central PMCID: PMCPMC7599417.
15. Li M, Song C, Dai M. The role of HIF signal mediated autophagy dysfunction in synovial fibroblasts in rheumatoid arthritis and the targeted regulation of kaempferol. Tissue Cell. 2026;98:103172. Epub 2025/10/08. doi: 10.1016/j.tice.2025.103172. PubMed PMID: 41056761.
16. Zhao Y, Yang J, Liao W, Liu X, Zhang H, Wang S, et al. Cytosolic FoxO1 is essential for the induction of autophagy and tumour suppressor activity. Nat Cell Biol. 2010;12(7):665–75. Epub 2010/06/15. doi: 10.1038/ncb2069. PubMed PMID: 20543840.
17. Tang H, Ma C, Xu M, Wu G, Li N, Chen L. SGK1 triggers cartilage degradation in TMJOA via FoxO1/autophagy. Arthritis Res Ther. 2025;27(1):231. Epub 2025/12/31. doi: 10.1186/s13075-025-03690-w. PubMed PMID: 41470005; PubMed Central PMCID: PMCPMC12754980.
18. Alarcón CR, Goodarzi H, Lee H, Liu X, Tavazoie S, Tavazoie SF. HNRNPA2B1 Is a Mediator of m(6)A-Dependent Nuclear RNA Processing Events. Cell. 2015;162(6):1299–308. Epub 2015/09/01. doi: 10.1016/j.cell.2015.08.011. PubMed PMID: 26321680; PubMed Central PMCID: PMCPMC4673968.
19. Zhang Y, Chen Y, Zhang J, Du X, Huang C. HNRNPA2B1 confers immune escape of non-small cell lung cancer through targeting lactate/ferroptosis. Cell Death Dis. 2025;17(1):49. Epub 2025/11/22. doi: 10.1038/s41419-025-08232-5. PubMed PMID: 41271615; PubMed Central PMCID: PMCPMC12811398 and consent to participate: This study had been approved by the Ethical Committee of Peking Union Medical College Hospital. Written informed consent was obtained from each patient for consent to participate. Consent for publication: All authors agree with the Consent for publication.
20. De Kesel J, Fijalkowski I, Pieters T, Borin C, Christensen KT, Wittouck M, et al. HNRNPC and m6A RNA methylation control oncogenic transcription and metabolism in T-cell leukemia. Blood. 2025;146(3):275–90. Epub 2025/05/28. doi: 10.1182/blood.2024026848. PubMed PMID: 40435411.

21. Zhang C, Chen Y, Sun B, Wang L, Yang Y, Ma D, et al. m(6)A modulates haematopoietic stem and progenitor cell specification. Nature. 2017;549(7671):273–6. Epub 2017/09/05. doi: 10.1038/nature23883. PubMed PMID: 28869969.
22. Hao L, Zhang W, Peng X, Bai Y, Tian C, Zhang Y, et al. Spermidine promotes osteogenic differentiation of BMSCs via the m(6)A methylation-autophagy axis under inflammatory stress. Free Radic Biol Med. 2026;245:301 – 16. Epub 2026/01/05. doi: 10.1016/j.freeradbiomed.2025.12.057. PubMed PMID: 41485545.
23. Zhang Y, Zhang J, Lin H, Wang J, Chen Q, Zhou T, et al. METTL3 and METTL14 determine human neural fate specifications. Nucleic Acids Res. 2025;53(22). Epub 2025/12/12. doi: 10.1093/nar/gkaf1397. PubMed PMID: 41385324; PubMed Central PMCID: PMCPMC12700100.
24. Levine B, Kroemer G. Biological Functions of Autophagy Genes: A Disease Perspective. Cell. 2019;176(1–2):11–42. Epub 2019/01/12. doi: 10.1016/j.cell.2018.09.048. PubMed PMID: 30633901; PubMed Central PMCID: PMCPMC6347410.
25. Lei X, Zhao G, Xie Y, Cui N. mTOR pathway mediates the endoplasmic reticulum stress -apoptosis of CD4 + T cell through inhibiting autophagy flux in sepsis. Inflamm Res. 2026;75(1):34. Epub 2026/02/07. doi: 10.1007/s00011-025-02114-4. PubMed PMID: 41653334; PubMed Central PMCID: PMCPMC12882968.

Figures

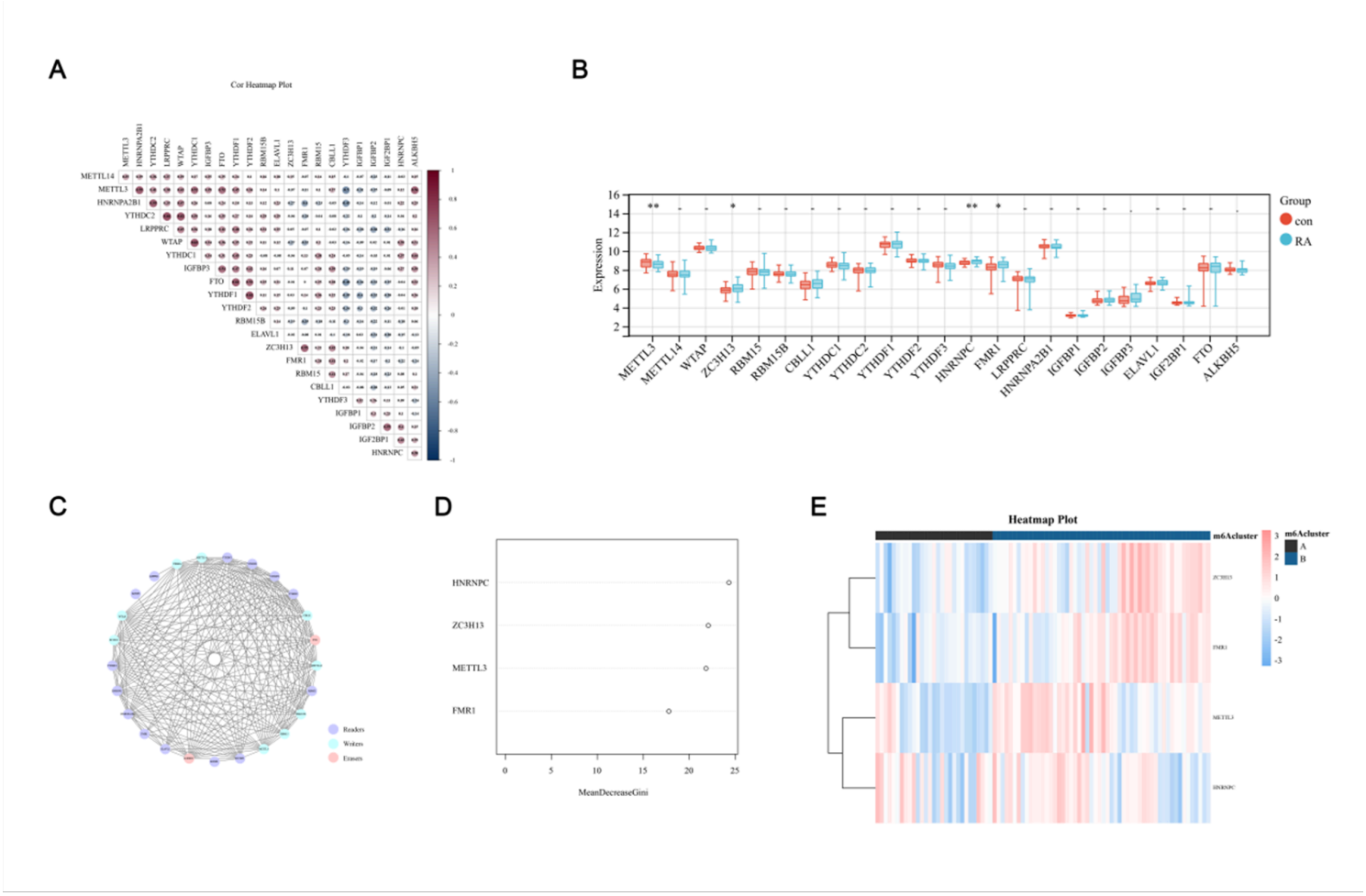


Figure 1

Bioinformatics analysis identifies HNRNPC as a key overexpressed m6A regulator in RA

(A) Spearman correlation heatmap and expression heatmap of 23 m6A regulators. (B) Boxplot of differentially expressed m6A regulators between RA and normal samples. (C) PPI network of 23 m6A regulators. (D) Feature importance ranking of m6A regulators in the RF model. (E) Hierarchical clustering heatmap of four key m6A regulators in RA and normal samples. Statistical analysis: Wilcoxon rank-sum test, $P < 0.001$, n=173.

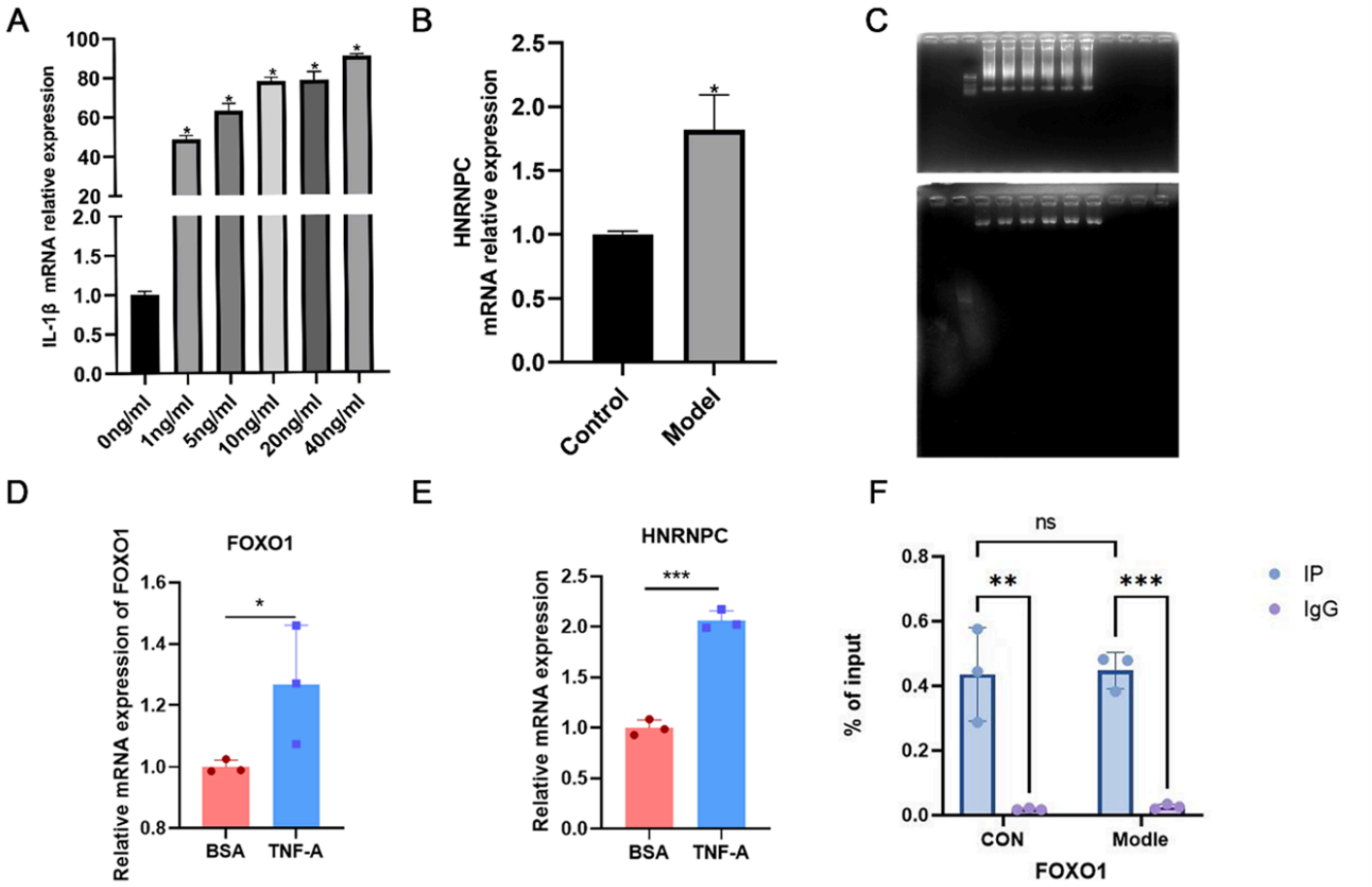


Figure 2

HNRNPC and FOXO1 are upregulated and FOXO1 m6A modification is enhanced in the RA cell model

(A) qPCR validation of IL-1B mRNA expression in the RA cell model. (B) TNF-αconcentration gradient experiment detecting HNRNPC mRNA expression. (C) RNA quality assessment for MeRIP-qPCR experiment. (D-E) Western blot detection of HNRNPC (D) and FOXO1 (E) protein expression. (F) MeRIP-qPCR detection of FOXO1 mRNA m6A modification level. Statistical analysis: Independent sample t-test (A, D, E, F), one-way ANOVA (B), n=3, $P < 0.01$, $P < 0.001$.

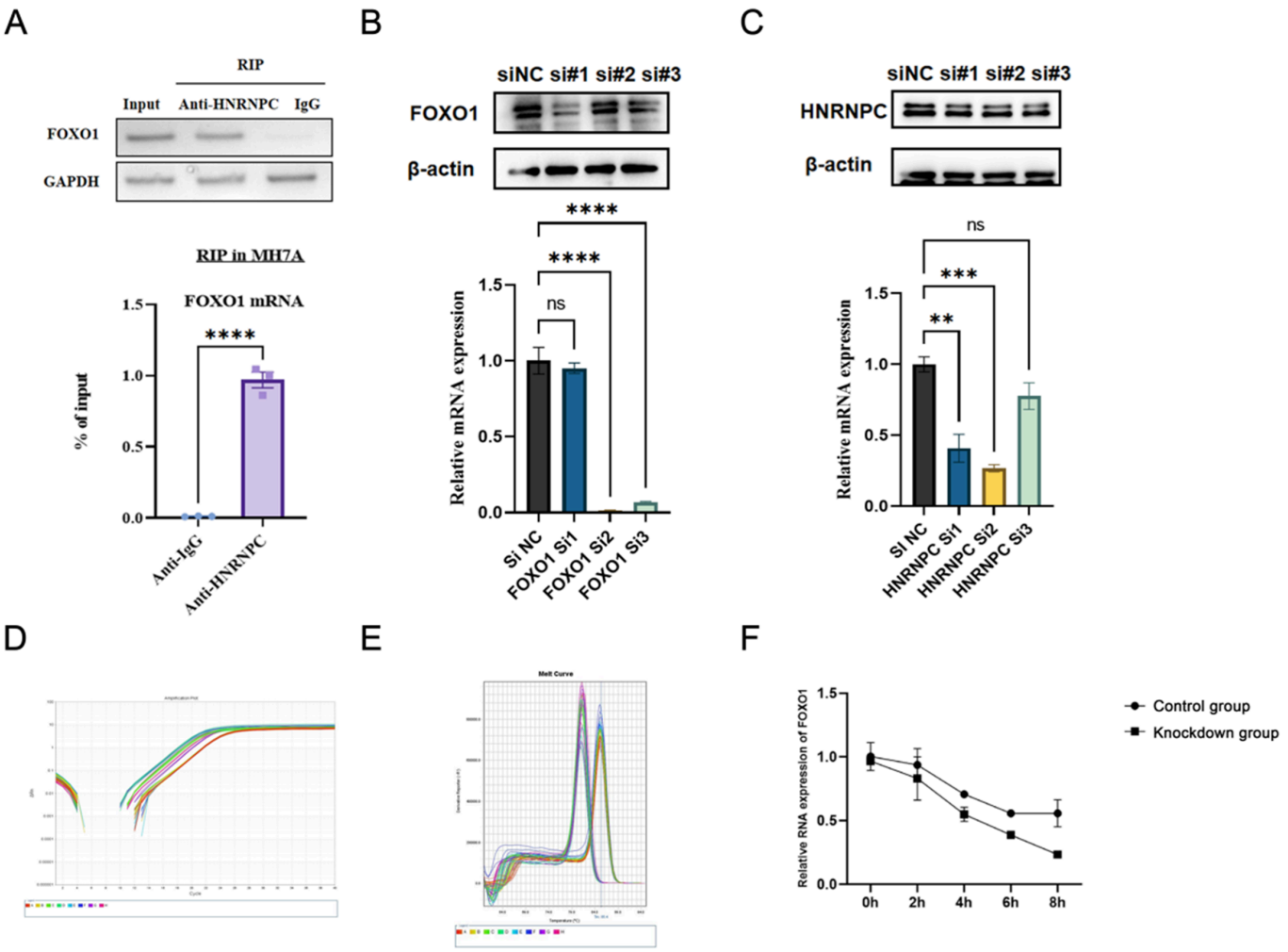


Figure 3

HNRNPC directly binds to m6A-modified FOXO1 mRNA and enhances its stability

(A) RIP-qPCR validation of the binding between HNRNPC and FOXO1 mRNA (Top: Electrophoresis bands; Bottom: qPCR quantification). (B-C) qRT-PCR detection of siRNA knockdown efficiency (B) and changes in FOXO1 mRNA expression (C). (D) FOXO1 mRNA decay curve. (E) Melt curves. (F) FOXO1 mRNA quantitative results at different time points. Statistical analysis: Independent sample t-test (A), one-way ANOVA (B, C), two-way ANOVA (D, F), n=3, $P < 0.01$, $P < 0.001$.

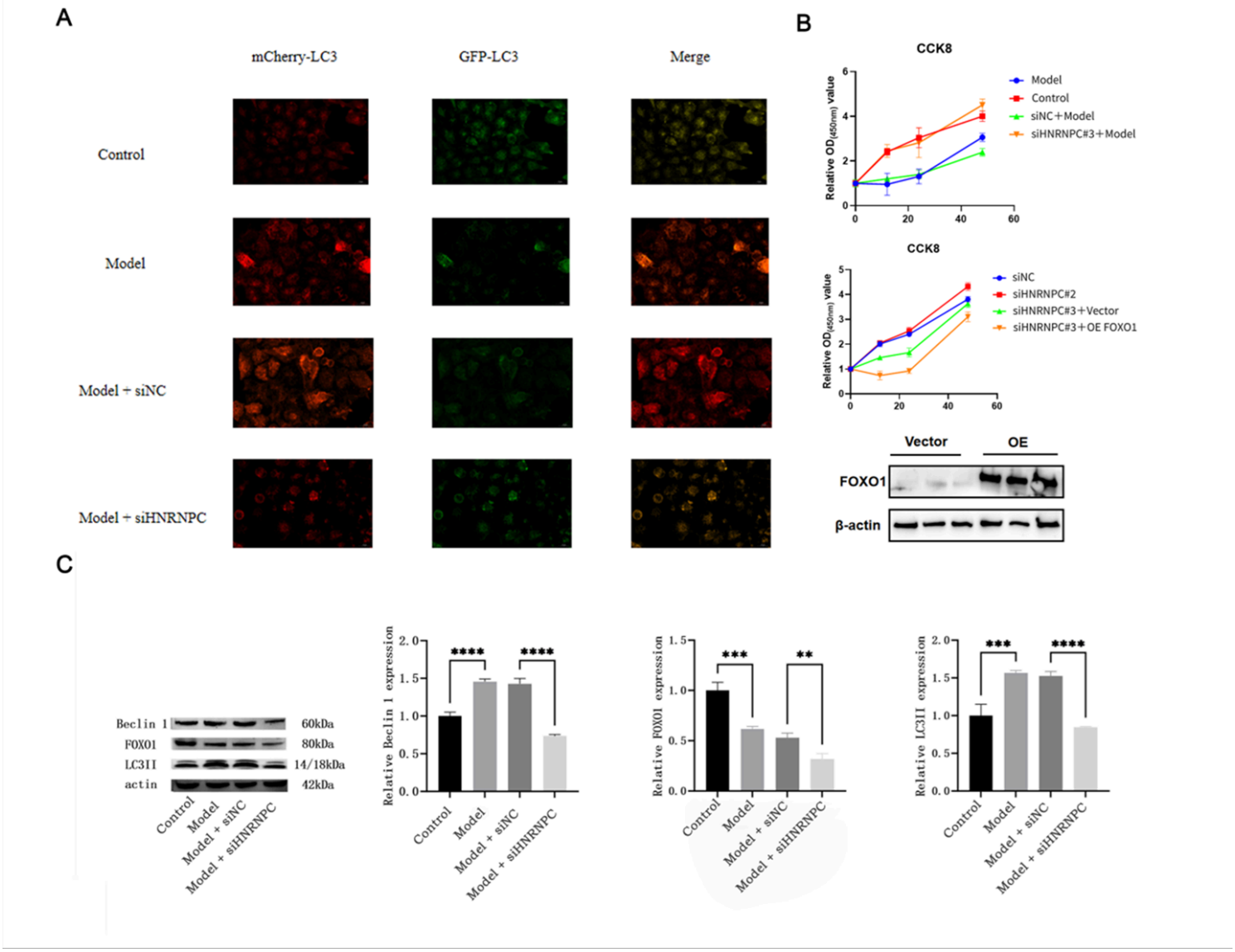


Figure 4

Knockdown of HNRNPC inhibits autophagy and abnormal proliferation in MH7A cells

(A) Immunofluorescence double-labeling for autophagic flux (mCherry-LC3/GFP-LC3). (B) CCK-8 assay for cell viability and the rescue effect of FOXO1 overexpression. (C) Western blot detection of autophagy-related protein expression. Statistical analysis: One-way ANOVA, n=3, $P < 0.01$, $P < 0.001$.

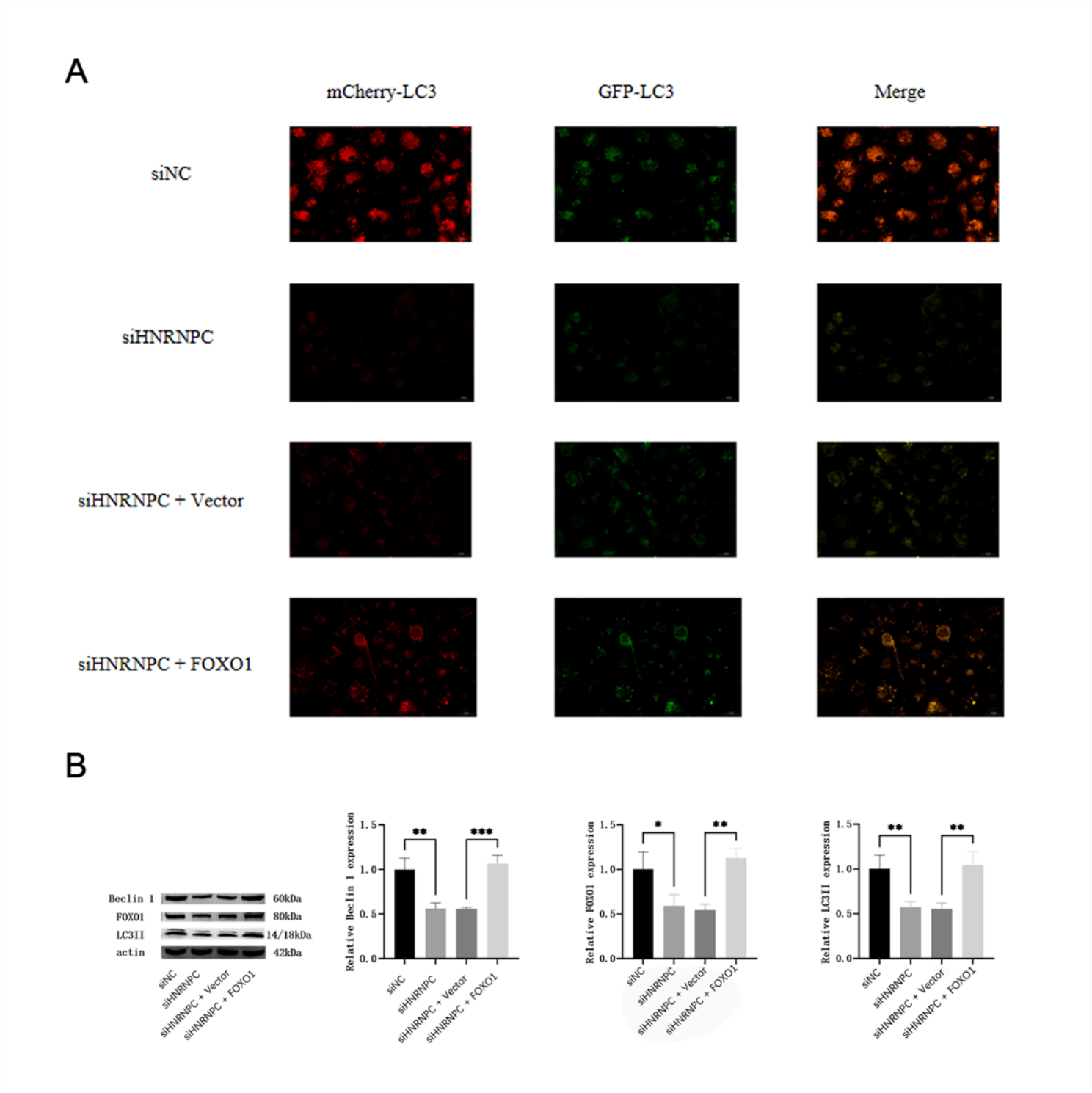


Figure 5

FOXO1 overexpression reverses autophagy inhibition caused by HNRNPC knockdown

(A) Immunofluorescence double-labeling for autophagic flux and statistical analysis of puncta counts. (B) Western blot detection of FOXO1 and autophagy-related protein expression in the rescue experiment. Statistical analysis: One-way ANOVA, n=3, $P < 0.01$, $P < 0.001$.

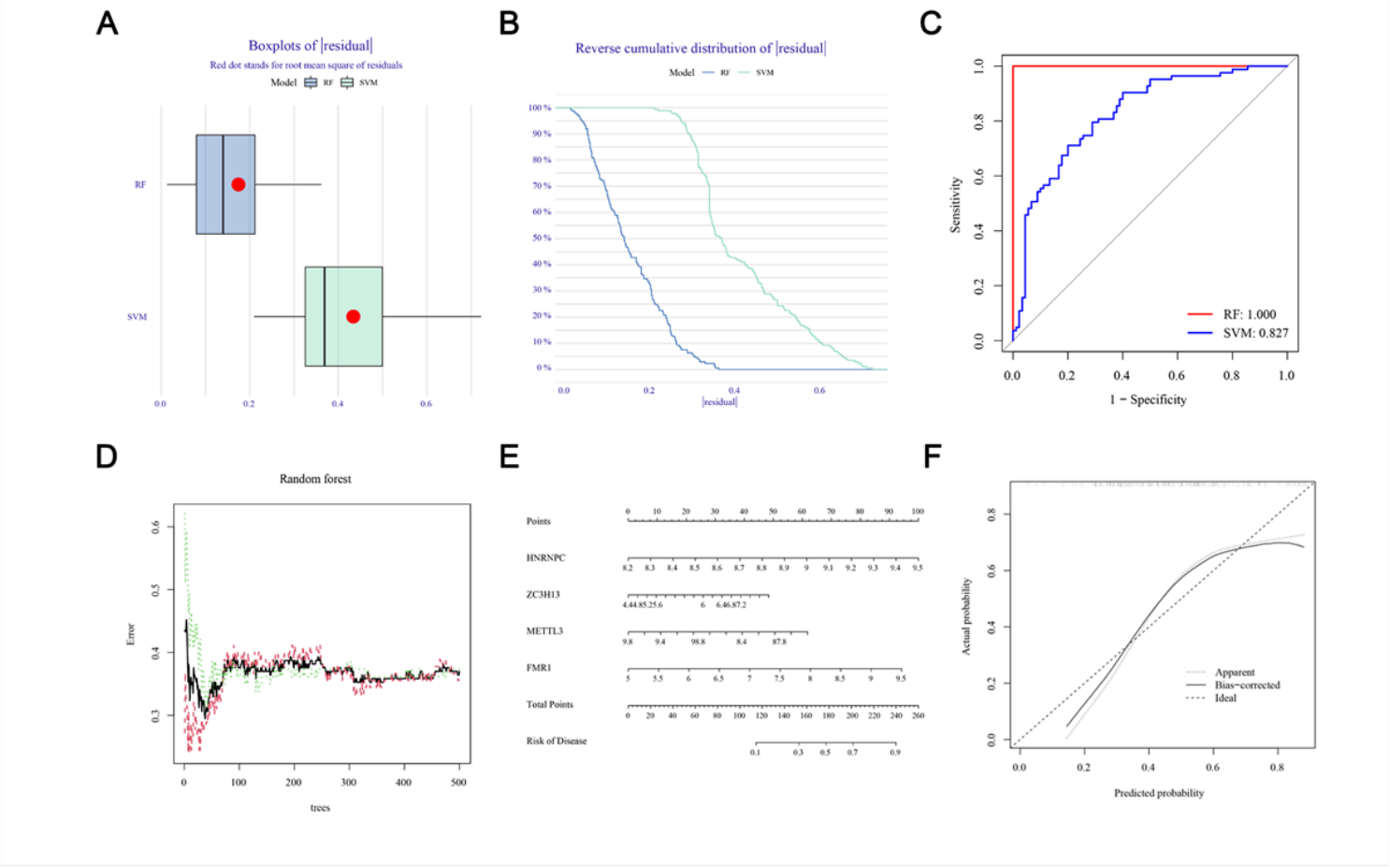


Figure 6

Validation of the importance of m6A regulators via machine learning

(A) Cumulative residual distribution plots for the Random Forest (RF) and Support Vector Machine (SVM) models.(B) Residual box plots for the RF and SVM models.(C) Comparison of receiver operating characteristic (ROC) curves for the RF and SVM models.(D) RF model error rate trend plot.(E) Nomogram diagnostic model based on four m6A regulators.(F) Calibration curve of the nomogram model.

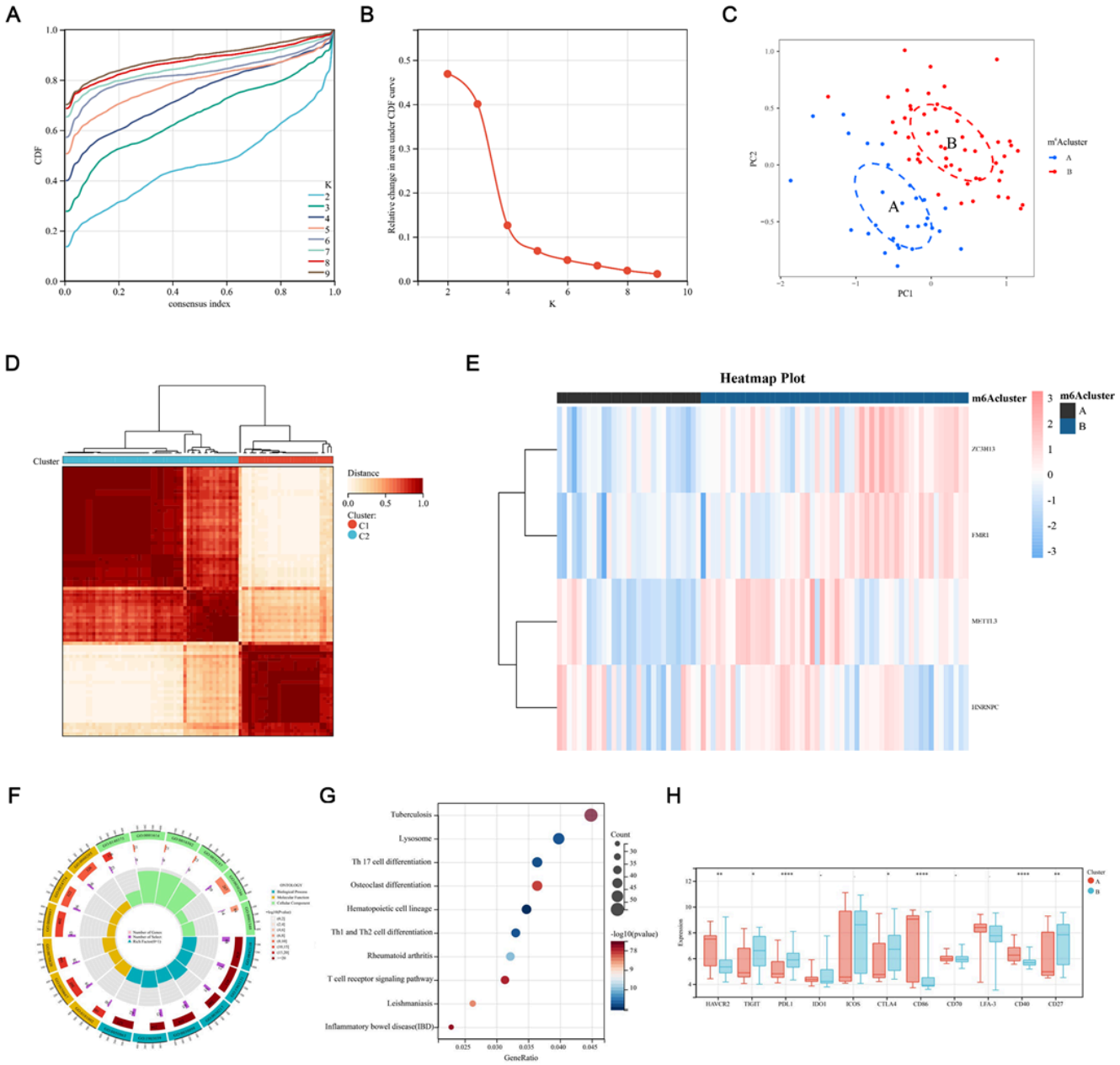


Figure 7

Identification of m6A modification subtypes and functional enrichment analysis

(A) Consensus clustering cumulative distribution function (CDF) curves (K=2-9). (B) Rate of change of the area under the CDF curve. (C) Principal component analysis (PCA) plot of different m6A subtypes. (D) Consensus matrix heatmap. (E) Expression heatmap of four key m6A regulators in different m6A subtypes. (F) Gene Ontology (GO) functional enrichment analysis of differentially expressed genes (DEGs). (G) Kyoto Encyclopedia of Genes and Genomes (KEGG) pathway enrichment analysis of DEGs.

(H) Expression heatmap of immune checkpoint inhibitors in different m6A subtypes. Statistical analysis: Wilcoxon rank-sum test, P < 0.001, n=173.

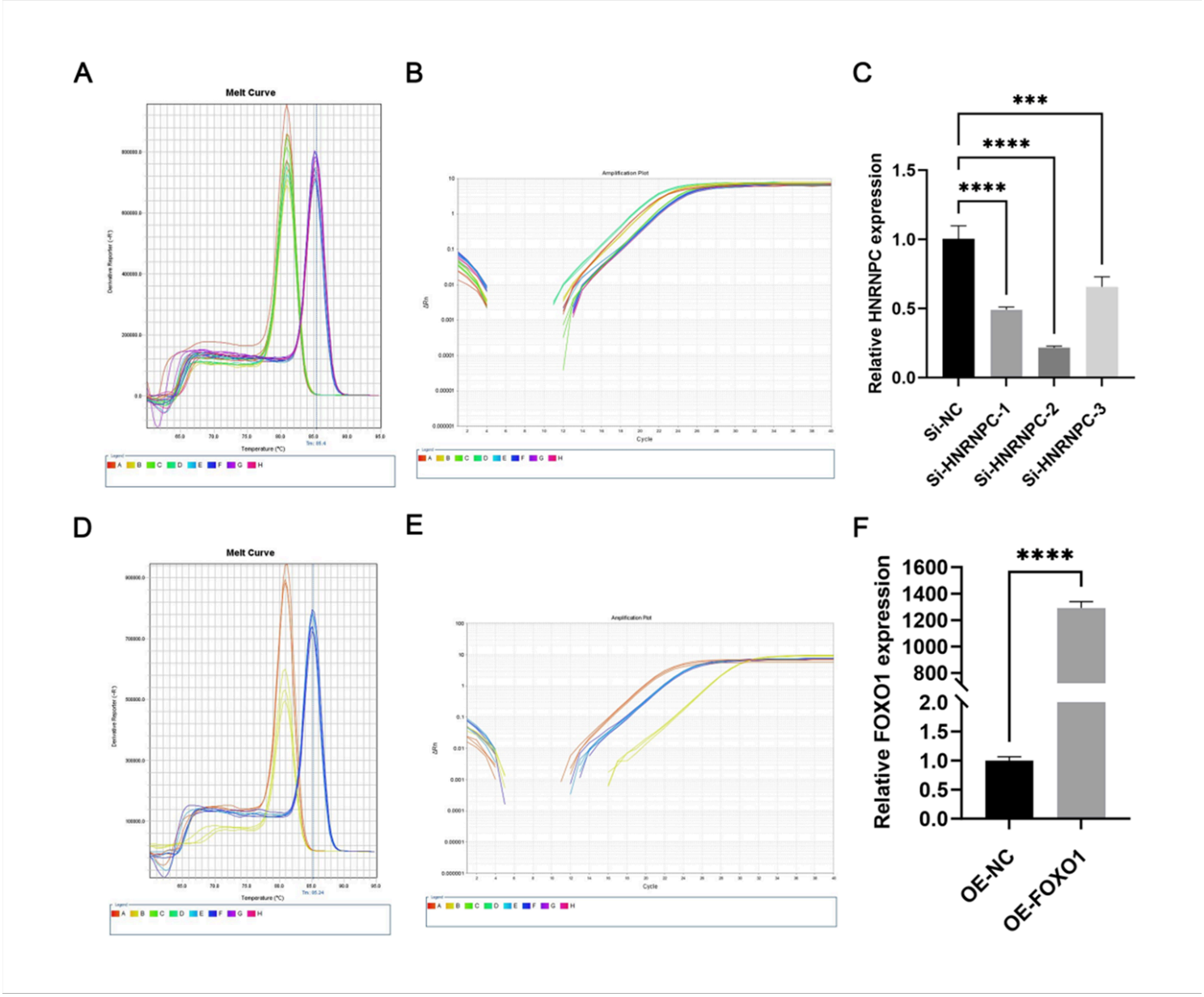


Figure 8

Validation of gene manipulation efficiency

(A-C) Quantitative real-time PCR (qRT-PCR) and melt curve analysis for the knockdown efficiency of small interfering RNAs targeting HNRNPC (si-HNRNPC).

(D-F) qRT-PCR and melt curve analysis for the overexpression efficiency of FOXO1. Statistical analysis: One-way analysis of variance (ANOVA) (A-C), Independent sample t-test (D-F), n=3, P < 0.001.

Supplementary Files

This is a list of supplementary files associated with this preprint. Click to download.

- SupplementPrimersequencesusedinthisstudy.docx